The Organization of Myosin and Actin in Rapid Frozen Nerve Growth Cones

P. C. Bridgman and M. E. Dailey

Department of Anatomy and Neurobiology, Washington University School of Medicine, St. Louis, Missouri 63110

Abstract. Rapid freezing and freeze substitution were used in conjunction with immunofluorescence, whole mount EM, and immunoelectron microscopy to study the organization of myosin and actin in growth cones of cultured rat superior cervical ganglion neurons. The general cytoplasmic organization was determined by whole mount EM; tight microfilament bundles formed the core of filopodia while a dense meshwork formed the underlying structure of lamellipodia. Although the central microtubule and organelle-rich region of the growth cone had fewer microfilaments, dense foci and bundles of microfilaments were usually observed. Anti-actin immunofluorescence and rhodamine phalloidin staining of f-actin both showed intense staining of filopodia and lamellipodia. In addition, staining of bundles and foci were observed in central regions suggesting that the majority of the microfilaments seen by whole mount EM are actin filaments.

Anti-myosin immunofluorescence was brightest in the central region and usually had a punctate pattern. Although less intense, anti-myosin staining was also seen in peripheral regions; it was most prominent at the border with the central region, in portions of lamellipodia undergoing ruffling, and in spots along the shaft and at the base of filopodia. Immunoelectron microscopy of myosin using postembedment labeling with colloidal gold showed a similar distribution to that seen by immunofluorescence. Label was scattered throughout the growth cone, but present as distinct aggregates in the peripheral region mainly along the border with the central region. Less frequently, aggregates were also seen centrally and along the shaft and at the base of filopodia. This distribution is consistent with myosins involvement in the production of tension and movements of growth cone filopodia and lamellipodia that occur during active neurite elongation.

THE organization of growth cone actin has been studied by light and electron microscopy (24, 25), but has not been correlated with growth cone morphology, which may relate to the speed of neurite elongation and the mode of growth cone advance (3). Although myosin has been detected by immunofluorescence in growth cones of neurons in primary culture (21, 34, 36) and PC12 cells (24), it is not clear how it is organized in relation to actin filaments and it has not been studied with immunoelectron microscopy. This is because of two problems associated with detecting myosin in growth cones of neurons grown in primary culture. First, myosin seems to be especially sensitive to fixation induced changes that cause the loss of antibody binding capacity. Second, growth cones themselves are especially sensitive to fixation-induced changes in their morphology. This means that mild fixation procedures that are required to maintain myosin antigenicity are not sufficient for good morphological preservation (21, 24). This has prevented a clear description of myosin organization and its structural interaction with actin in growth cones of cultured neurons.

To overcome these problems we have adapted freezing and freeze substitution procedures that circumvent both the distortion of growth cone morphology and loss of antigenicity by myosin. This has allowed us to use immunofluorescence and immunoelectron microscopy under conditions that potentially give a more accurate description of growth cone structure, as well as myosin and actin organization.

An accurate description of actin and myosin organization may be important because there is considerable evidence that the production of tension by the growth cone is somehow involved in either the elongation process or guidance (4, 6, 23). The mechanism for tension production is thought to occur through the interaction of actin and myosin (reviewed in reference 26). Although recent work on Aplysia neurons and PC12 cells using video-enhanced DIC (1, 15) has challenged whether tension is important for neurite elongation, this does not necessarily mean that actin-myosin interaction may not be important for some aspect of growth cone motility or guidance that leads to directed neurite growth. For example, depolymerization of growth cone actin greatly slows neurite elongation and causes disorientation of the growth (28). Uncertainties related to how actin is producing its effect on neurite growth suggest that a closer look at myosin and actin organization in growth cones is warranted.

© The Rockefeller University Press, 0021-9525/89/01/95/15 $2.00

Materials and Methods

Cell Culture

The culture methods for rat superior cervical ganglion neuron explants or dissociated cells were the same as has been described previously (18) except laminin (Collaborative Research, Inc., Waltham, MA) was used as the adhesive substrate. Laminin-coated coverslips were prepared by the method described by Rogers et al. (33).

Freezing

Freezing was done one of three ways depending on the purpose for which the specimen was to be used. (*a*) Immunofluorescence: Explants were grown on 22 × 22-mm coverslips. Immediately before freezing the coverslips were removed from an adjacent incubator, picked up with forceps, blotted once to remove excess culture medium, and then plunged quickly by hand into a stirred mixture of propane/ethane (3:1) cooled to ~−190°C by liquid nitrogen. The delay between removal from the incubator to the point of freezing was 10–20 s. (*b*) Whole mounts: Explants were grown on gold EM grids coated with formvar. They were removed from the incubator, rinsed with warm L-15, quickly blotted of excess fluid, and then frozen rapidly by spring driven entry (at >3 M/s) into a stirred mixture of propane/ethane (3:1; −190°C; reference 8). (*c*) Thin sections: Explants were grown on 4-mm glass disks. They were mounted on the freezing head of a Heuser/Reese type "slam" freezing machine, blotted free of excess fluid, and frozen rapidly by dropping on to a polished copper block cooled by liquid helium (17). To prevent retraction of growth cones that can be induced by precooling of specimen by the cold helium vapor, the specimen were protected by a foam cap until just before dropping onto the copper block.

Freeze Substitution

Three different freeze substitution protocols were used depending on the method of freezing and the purpose for which the specimen were to be used. (*a*) Immunofluorescence: The coverslips containing explants that had been stored in liquid nitrogen were transferred directly to −80°C methanol containing 1% formaldehyde. The methanol/formaldehyde solution was allowed to warm over a 30-min period to −20°C in a standard freezer. The samples were then rehydrated by transfer to PBS at room temperature. (*b*) Whole mounts: The procedure was as previously described (8). Briefly, this entailed substitution in acetone containing the following sequence of fixatives: 10% acrolein, 0.2% osmium, and then 10% glutaraldehyde. Staining was with 0.5% uranyl acetate and 0.5% hafnium chloride. (*c*) Thin sections: Samples were substituted at −80°C in acetone containing 0.1% uranyl acetate (anhydrous) for 24 h. They were then warmed to −70°C and rinsed three times with acetone and three times with methanol.

Antibody Labeling for Immunofluorescence

Freeze substituted, rehydrated cells were incubated with primary antibodies to chicken gizzard actin (rabbit anti-actin; Biomedical Technologies, Inc., Cambridge, MA) or human platelet myosin (rabbit anti-myosin; Biomedical Technologies, Inc.) at a 1:10 dilution for 1 h. They were rinsed three times and then incubated with the appropriate rhodamine-conjugated secondary antibody (Organon Teknika-Cappel, Malverne, PA) at a 1:400 dilution for 45 min. For labeling microtubules, a rabbit antiserum against sea urchin tubulin (Polysciences, Inc., Warrington, PA) was used at a 1:50 dilution. The secondary antibody was conjugated to fluorescein and was used at a 1:500 dilution. The labeling procedure was that described by Terasaki et al. (38).

Rhodamine-Phalloidin Staining

Cells were fixed with a warm solution containing 0.25% glutaraldehyde in 0.1 M sodium cacodylate buffer, pH 7.4. They were then incubated with a solution containing 0.2% saponin and 0.33 μM rhodamine phalloidin (Molecular Probes, Eugene, OR) in buffer for 5 min, rinsed, and mounted for observation.

Immunofluorescence Microscopy

Stained cells were viewed and photographed with Tri X or T Max Film (Eastman Kodak Co., Rochester, NY) on a Zeiss IM-35 microscope using a 63× planapo or 100× Neofluor lens.

Preparation for Electron Microscopy

Whole Mounts. After freeze substitution, grids containing explants were critical-point dried as previously described (8) and then coated with a thin layer of carbon.

Embedment in K11M and Postembedment Antibody Labeling. The procedure used was the new Lowicryl low temperature resin K11M (Polysciences, Inc.; 11). Samples were infiltrated at −60°C according to the following schedule: (*a*) 1:1 acetone/K11M for 24 h; (*b*) 1:2 acetone K11M for 24 h; (*c*) 100% K11M (two changes) for 24 h. Samples were then placed in shallow aluminum dishes containing fresh K11M and covered tightly with plastic wrap. Polymerization of the K11M with UV light was done gradually to prevent buildup of heat that may occur during the exothermic reaction (2). The following schedule was used: (*a*) 24 h at −70°C; (*b*) 48 h at −60°C; (*c*) 24 h at −40°C; (*d*) 48 h at −20°C; and (*e*) 24 h at room temperature.

Antibody labeling: (*a*) Thin sections were picked up on formvar-coated nickel grids; (*b*) sections were incubated for 30 min with 10% horse serum + 4% BSA in TBS + Tween 20 (TBST[1]; 10 mM Tris-HCl, pH 8.0, 500 mM NaCl, 0.05% Tween 20); (*c*) sections were washed for 30 s with TBST; (*d*) sections were then incubated with the antiserum for 1 h (diluted 1:10 in TBST + 1% BSA); (*e*) sections were washed twice (1 min each) with TBST; (*f*) final incubations were with goat anti-rabbit (1:20) or protein A (1:20) conjugated to 10 nm colloidal gold (Janssen Life Science Products, Piscataway, NJ) for 30–45 min; (*g*) sections were washed for 1 min and then dried in a vacuum desiccator; (*h*) they were then grid stained with uranyl acetate (0.5% in 50% methanol, 10–15 min) and/or potassium permanganate (1% in PBS, 30–60 s under nitrogen atmosphere; if double stained, grids were vacuum dried between stains).

Electron Microscopy

Whole mounts were viewed at 100 KV in a JEOL 100CX-11 or at 1000 KV in an A.E.I. EM-7. Thin sections were viewed at 80 KV in a JEOL 100CX-11.

Results

Specificity of Antisera

The anti-human platelet myosin antiserum was designated by the manufacturer to be specific for the vertebrate nonmuscle myosin heavy chain. It was reported to contain no detectable cross reactivity with any other protein including skeletal, smooth, or cardiac muscle myosin. Immunoblots of purified human platelet myosin confirmed that it reacts with both the intact heavy chain and the portion of the heavy chain that makes up the rod portion of the myosin molecule (Fig. 1). To insure that the antiserum showed specific cross-reactivity with rat superior cervical ganglion (SCG) nerve myosin, immunoblots were also performed on whole SCG protein. Only a single band at 205 kD could be detected, suggesting that the antiserum reacts primarily if not only with the heavy chain of rat nerve myosin (Fig. 1).

The anti-actin antiserum was raised against purified chicken gizzard actin and was reported by the manufacturer to be specific for G and F actin from both muscle and nonmuscle cells of vertebrates and invertebrates. The fluorescence staining pattern in rat fibroblasts was consistent with that expected for actin; stress fibers and lamelli stained intensely (data not shown). Control preparations showed no staining.

The anti-tubulin antiserum was against sea urchin tubulin. In rat fibroblasts it showed a pattern of staining characteristic of microtubules (data not shown).

1. *Abbreviations used in this paper*: SCG, superior cervical ganglion; TBST, Tris-buffered saline + Tween 20.

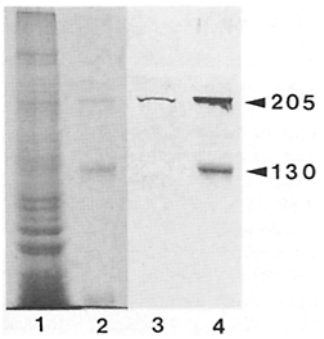

Figure 1. The specificity of the anti-human platelet myosin antiserum determined by immunoblot. Lane *1* shows the Coomassie Blue-stained 7% gel of whole SCG protein separated by SDS-PAGE. The stock crude whole protein solution loaded onto the gel was prepared by homogenization of 40 decapsulated SCG in 120 μl of buffer, pH 7.0, of the following composition: 15 mM sodium pyrophosphate, 5 mM $MgCl_2$, 3 mM DTT, 30 mM imidazole chloride, 10 mM EDTA, 0.1 mM PMSF, 10 mg/ml aprotinin. Lane *2* shows the Coomassie Blue-stained 7% gel of purified platelet myosin. The myosin was purified according to the procedures of Pollard et al. (32) as modified by Peleg et al. (30). Two major bands are seen. The first at 205 kD represents the intact myosin heavy chain while the second at 130 kD represents a degradation product of the heavy chain (lacking the portion of the heavy chain that makes up the head of the myosin molecule) that is commonly seen in these preparations. Lanes *3* and *4* represent the Western blot of the gel prepared using a phosphatase reaction product detection system and Zeta-Probe membranes (Bio-Rad, Richmond, CA). Lane *3* is the whole SCG protein which shows only a single reactive band at 205 kD. Lane *4* is the purified platelet myosin which shows reaction of both major bands at 205 and 130 kD.

General Morphology of Growth Cones

Rapid frozen, freeze-substituted whole mounts provided a good means for observing the overall organization and three-dimensional structure of intact growth cones. In our analysis we focused upon relatively large growth cones that showed broad peripheral expansions because these tend to be associated with the most rapidly elongating neurites in our culture system. Each explant in our culture system produces large numbers of readily observable growth cones. The observations are thus compiled from >300 images of individual growth cones from 15 different preparations. In EM stereo pairs it was apparent that the base or initial expansion of the growth cone from the neurite was usually thick relative to the remaining more thinly spread area. The base usually contained mitochondria, dense core vesicles, clear vesicles, and a network of membranous tubules (Fig. 2). Microtubules were numerous as they splayed out from the neurite into the expansion. To identify this region of the growth cone we will use the terminology that was introduced for the description of distinct cytoplasmic regions in rapid frozen fibroblasts (10) and that has recently been extended to the description of growth cones derived from Aplysia neurons (14). This organelle and microtubule-rich region will be referred to as the central or C domain. The surrounding thinly spread region of the growth cone will be referred to as the peripheral or P domain. The P domain was usually devoid of organelles and was penetrated by only a few microtubules. Depending upon whether the P domain contained distinct filopodia, the organization of microfilaments differed. If filopodia were present, then the P domain contained distinct tight bundles of microfilaments which formed the core of the filopodia (Fig. 2 *A*). The proximal ends of many of the bundles ended at the boundary between the P and C domain although occasionally bundles did extend into the C domain. A meshwork of microfilaments extended between the microfilament bundles and were especially dense within lamellipodia or veils that spread between filopodia. If the growth cone completely lacked filopodia at the leading edge then distinct bundles of microfilaments were usually not detectable, although often within such broadly spread lamellipodia there were some less precisely aligned, loose bundles containing several filaments (Fig. 2 *B*). Most of the lamellipodia contained an overlapping meshwork of filaments that were roughly oriented so that they extended from the periphery towards the C domain similar to the orientation of the microfilament bundles in growth cones with filopodia. In stereo images it was apparent that both filopodia and lamellipodia were sometimes raised above the substrate, indicating that they probably were only loosely adhesive and frozen during movements.

In some growth cones the ends of microfilament bundles terminated in distinct mounds that appeared to represent aggregations of microfilaments (Fig. 3). The size of these aggregations or foci varied; sometimes they were relatively small and did not form a distinct mound (Fig. 3 *B*), while in other instances they were large and seemed to project upward in a manner that resembled a nascent filopodium (see Fig. 2). Most growth cones had between 3 and 10 aggregations. The relationship between microfilament bundles and the aggregations was complex because the aggregations could also exist in completely lamellipodial growth cones without distinct microfilament bundles in the P domain.

To determine whether the microfilaments observed in whole mounts were actin filaments, fluorescence staining with the F actin-specific toxin, rhodamine-phalloidin was performed. The thin P domain of the growth cone, whether it contained filopodia or lamellipodia, stained intensely. When observing the pattern of stain by eye in the microscope the bright staining in the lamellipodia often appeared as a sheet of filaments roughly oriented with one end at the leading edge. Because of the extreme brightness of these areas the staining appeared to be almost homogeneous in photographs (Fig. 4, *A–C*). In any case, the brightness of the staining indicates a very high concentration of actin filaments. The central region also stained but the pattern was much more variable. In most cases numerous distinct lines transected the C domain which presumably represent bundles of actin filaments (Fig. 4, *A* and *B*). Less frequently the C domain was almost devoid of any staining except along the border where there was a transition into the P domain (not shown). The transition regions usually contained lines of stain which probably represent actin bundles. In many instances the transition zone and C domain also contained very bright spots of staining which may represent discrete actin filament aggregations (Fig. 4, *A* and *B*). These staining patterns were consistent with the range of distribution of microfilaments seen in the rapid frozen whole mounts. We therefore assume that the majority of the microfilaments that are observed in whole mounts, including those that form the distinct filament aggregates or foci, represent actin filaments.

In contrast to the staining pattern seen with rhodamine-

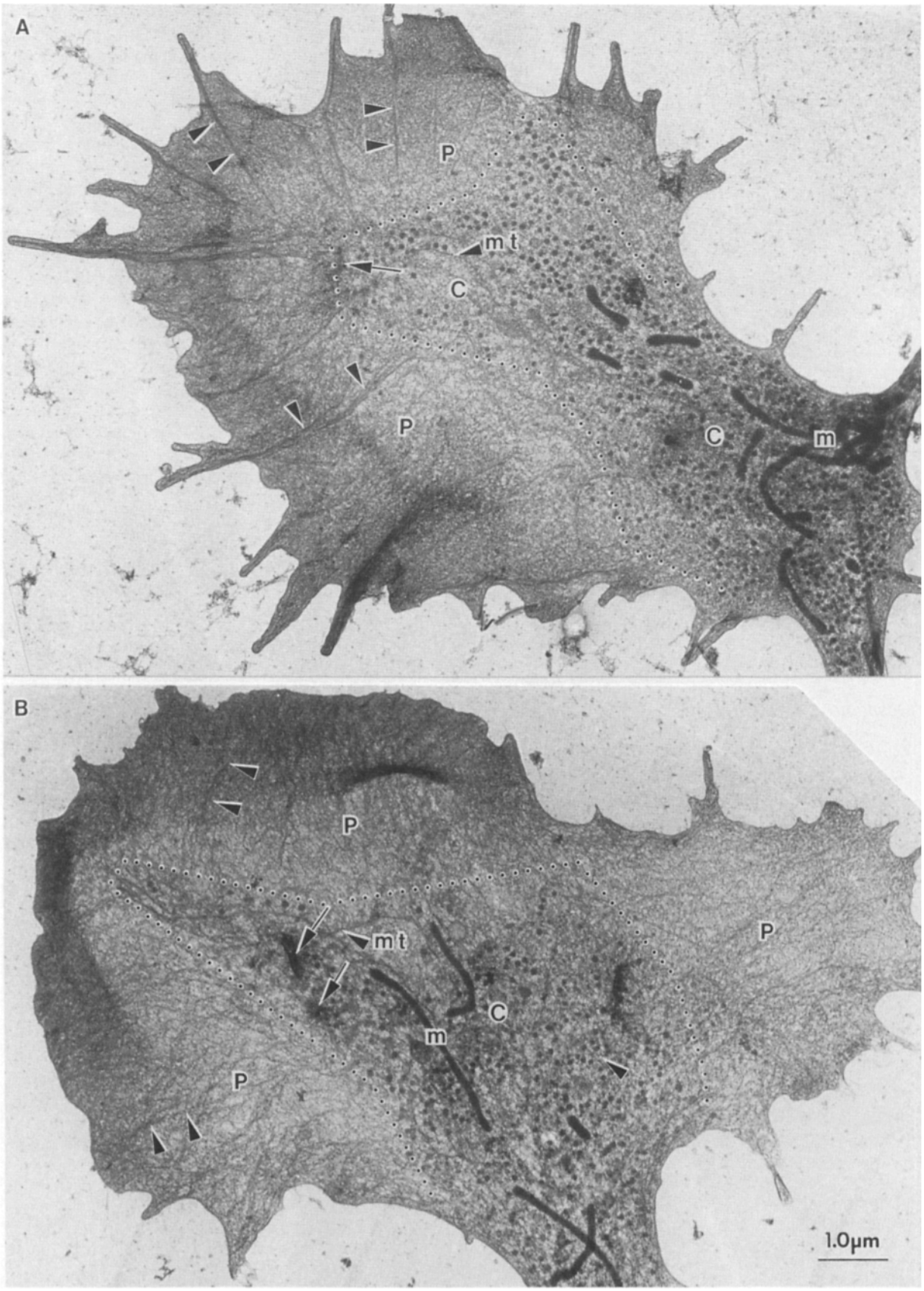

Figure 2. Whole mount electron microscopy of growth cones prepared by direct rapid freezing and freeze substitution. (*A*) The overall structure of a typical mixed lamellipodial/filopodial type growth cone is depicted. Two distinct cytoplasmic domains are present. The approximate boundary between the two domains is shown by the dotted line. The central (*C*) domain contains microtubules (*mt*), mitochondria

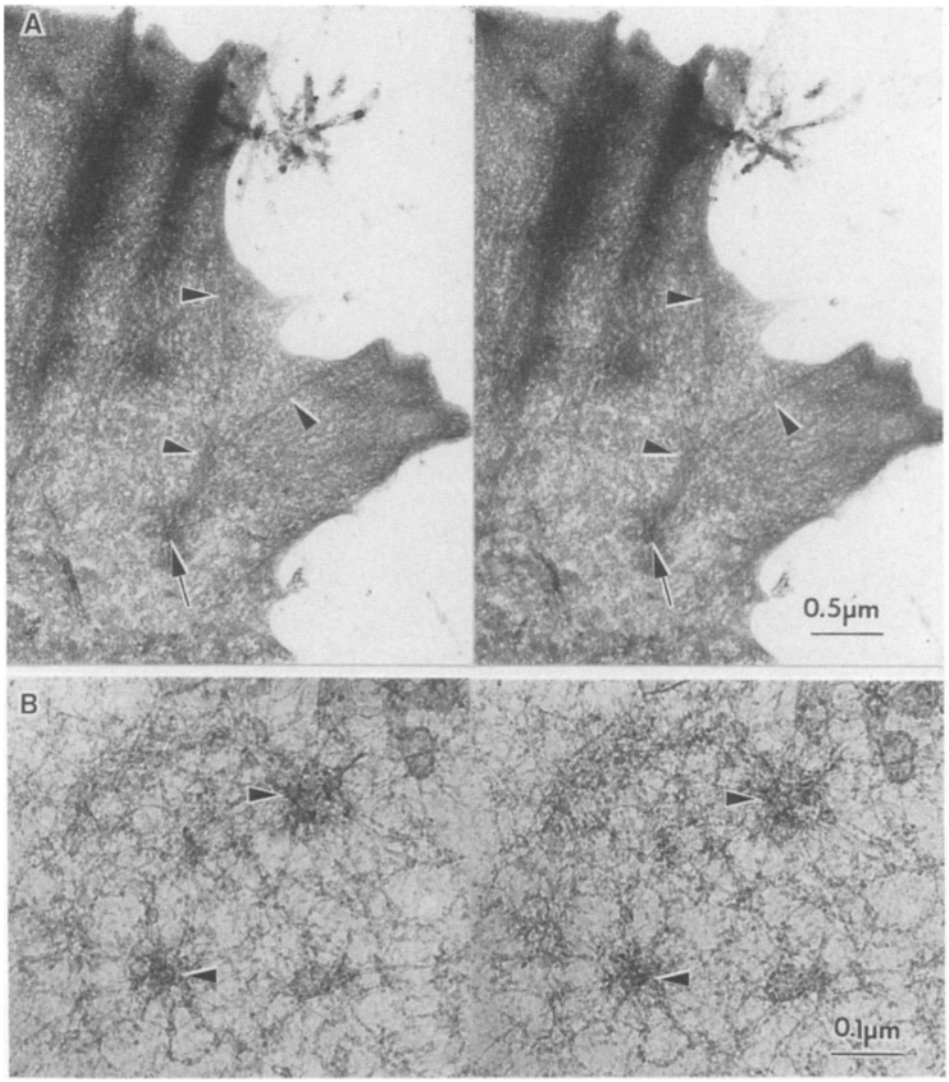

Figure 3. (*A*) A whole mount EM stereo view of a portion of growth cone lamellipodia. Bundles of microfilaments (*arrowheads*) terminate in a dense foci (*arrow*). The cytoplasm of this cell is slightly reticulated due to ice crystal formation during the freezing. This tends to obscure the filaments that make up the meshwork but has little effect on the visualization of bundled microfilaments. (*B*) A higher magnification stereo view of two foci (*arrowheads*) in a growth cone from a fixed whole mount preparation. Fixed cells had less densely staining granular material that tends to obscure filaments than directly frozen, freeze-substituted cells. Microfilaments appear to connect to a dense material at the foci.

phalloidin, immunofluorescence staining of microtubules showed that they were most concentrated in the C domain (Fig. 4 *D*). As microtubules left the neurite they splayed out in a variety of patterns. Sometimes the microtubules were only slightly curved and a few penetrated into the P domain; rarely they extended all the way to the growth cone margin. In such cases they often seemed to align with actin filament bundles (compare Fig. 4, *C* and *D*). Sometimes microtubules were distinctly bent in tight but smooth curves or were looped and stayed within the C domain. The immunofluorescence images of microtubules were especially useful in determining the pattern of microtubules at the thick base of the growth cone where the superimposition of organelles and cytoplasmic material made the identification of microtubules in whole mounts more difficult. The pattern observed by immunofluorescence was consistent with and complemented that which was observed in the rapid frozen whole mounts.

Immunofluorescence of Actin and Myosin

Immunofluorescence staining of frozen, freeze-substituted growth cones using antibodies against actin gave a staining

(*m*), and numerous dense core vesicles. The peripheral (*P*) domain contains distinct microfilament bundles (*arrowheads*) that form the core of the majority of filopodia. A meshwork of microfilaments fills the cytoplasm between the filament bundles in the peripheral domain. Some of the microfilament bundles appear to terminate in discrete areas (*arrow*) that stain darkly compared to the surrounding cytoplasm. (*B*) A typical pure lamellipodial type growth cone (no filopodia at the leading edge) is shown. The C domain has the same characteristics as indicated for the growth cone shown in *A*, while the P domain differs in two respects (the boundary between the two domains is indicated by the dotted line). Filopodia are not present at the leading edge and distinct tight bundles of microfilaments are not seen. The meshwork of microfilaments within the lamellipodia is organized with approximately the same orientation as the tight bundles; microfilaments extend from the leading edge towards the C domain. Although distinct tight bundles of microfilaments are not seen, some looser bundles of several microfilaments are seen integrated within the meshwork (*arrowheads*). Dense aggregates of microfilaments are also seen (*arrows*), but it is not obvious whether the filaments in the P domain terminate at these points.

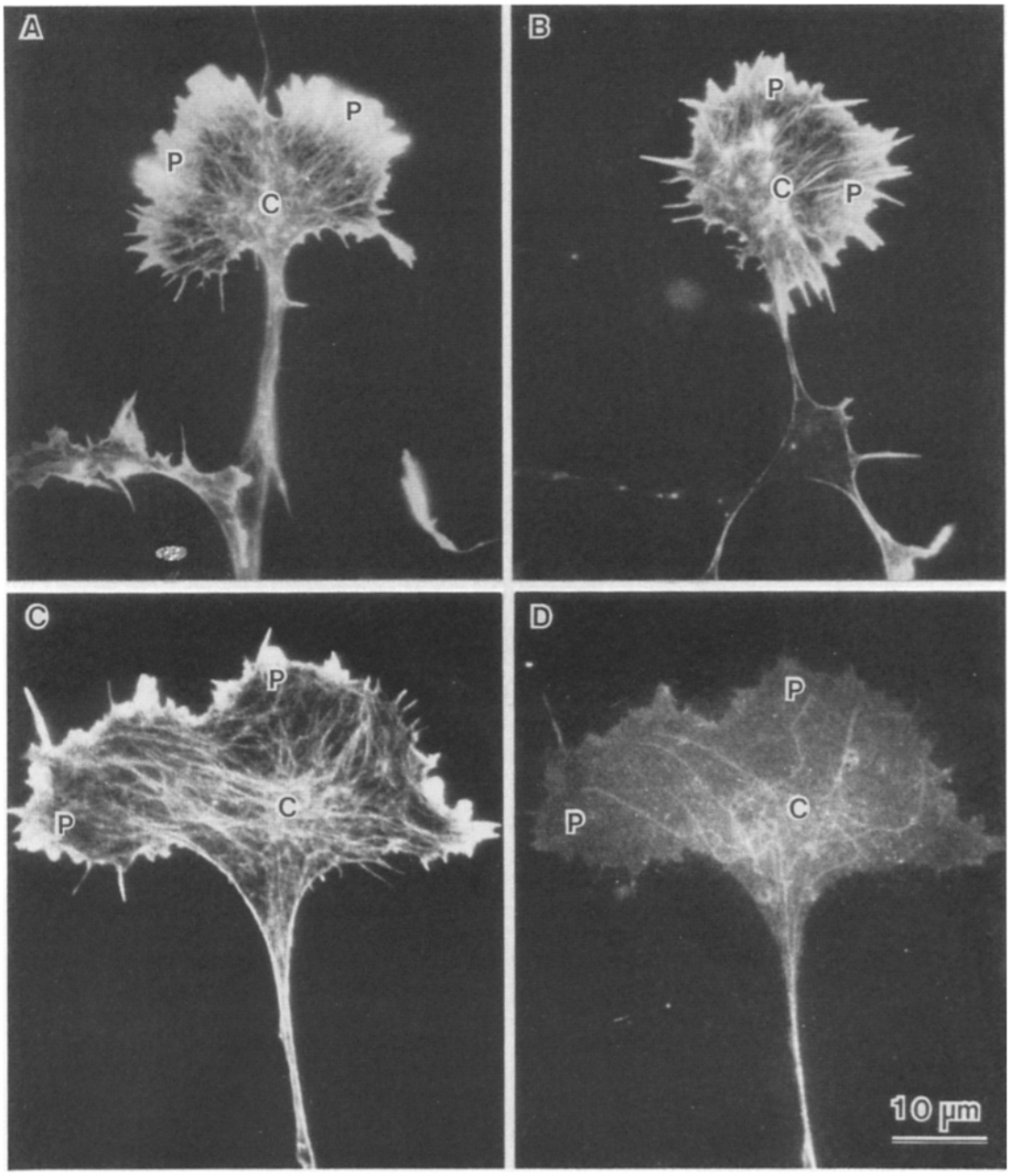

Figure 4. The distribution of actin filaments in growth cones as shown by rhodamine-phalloidin staining (*A–C*) and microtubules detected by immunofluorescence (*D*). (*A* and *B*) The peripheral domain stains very brightly for actin while the central domain stains less intensely. The staining in the P domain appears uniform while the stain in the C domain appears as distinct lines that probably indicate bundles or spots that may represent aggregations or foci. (*C* and *D*) Double staining of a single growth cone. The distribution of actin is shown by rhodamine-phalloidin staining (*C*) and compared to the distribution of microtubules detected by immunofluorescence using a fluorescein secondary antibody (*D*). Microtubules splay out from the neurite in the C domain and often loop or make relatively tight S turns. Some microtubules penetrate into the P domain and occasionally extend almost all the way to the edge. Actin filaments and microtubules often seem to be aligned in the P domain and in transition zone between the two domains. *P*, peripheral domain; *C*, central domain.

pattern similar but not identical to that seen with rhodamine-phalloidin. The observations are based upon 93 images of individual growth cones from four separate preparations. Typically (in 87% of the growth cones observed) the brightest staining was again seen in lamellipodia and filopodia (Fig. 5, *A* and *B*). However, unlike the pattern seen with the rhodamine-phalloidin, the brightly stained areas appeared homogeneous both to the eye and in photographs. Similar to the rhodamine-phalloidin staining, the C domain stained less brightly than the P domain. The C domain also tended to have lines of stain that probably represent actin bundles, although this was less obvious than in the rhodamine-phalloidin–stained growth cones. In addition, neurites stained much more intensely than with rhodamine-phalloidin. These dif-

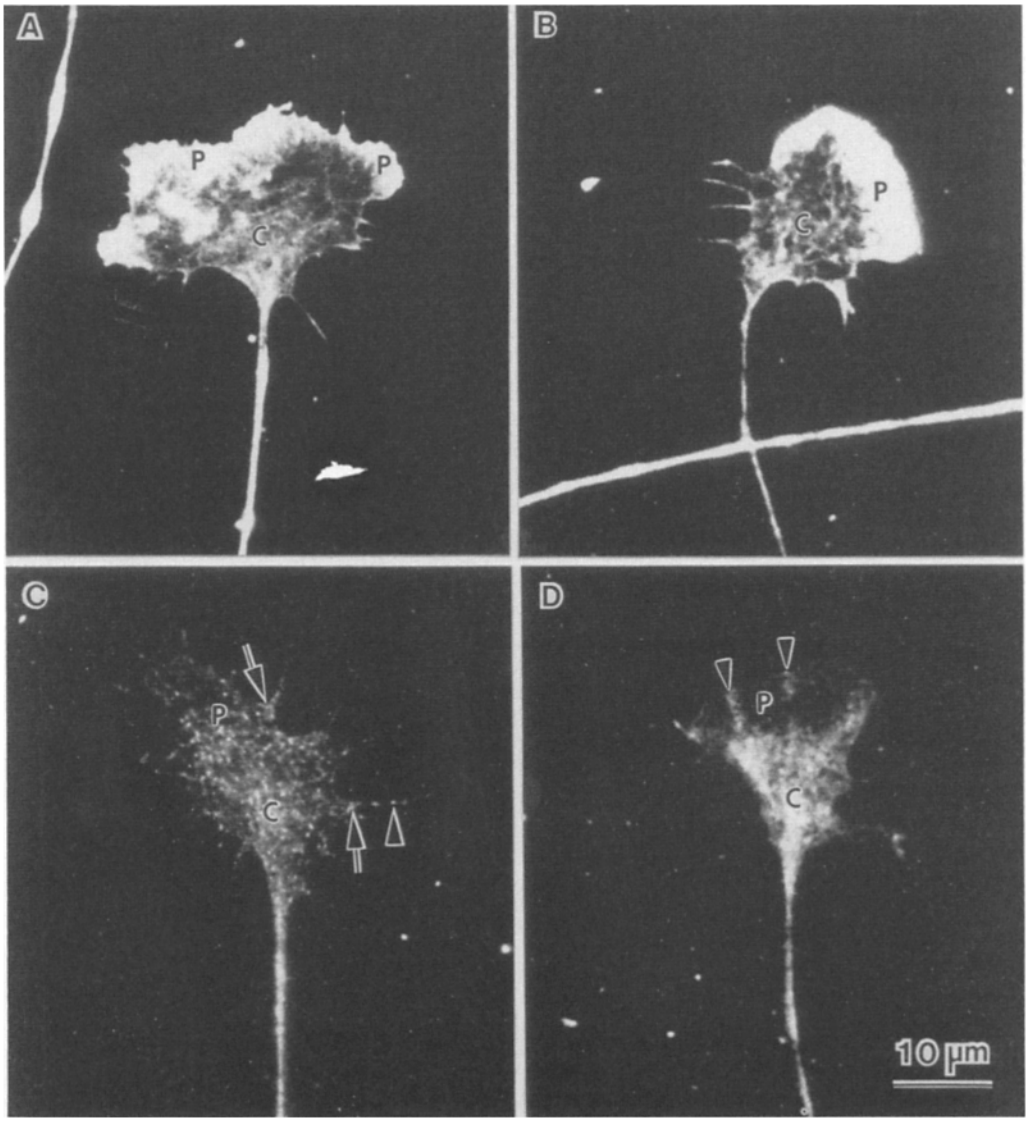

Figure 5. Immunofluorescence of actin (*A* and *B*) and myosin (*C* and *D*) in frozen, freeze-substituted growth cones. (*A* and *B*) The actin staining is similar to that seen with rhodamine-phalloidin; the P domain is intensely stained compared to most of the C domain. Occasionally the C domain contains bright spots of stain. However, neurites stain brighter than with rhodamine-phalloidin. (*C* and *D*) The myosin staining is brightest in the C domain and is often punctate when precisely focused (*C*). Staining is also bright in the transition zone between the P and C domains. Small spots of stain can be seen distributed throughout the P domain and are especially bright at the base of some filopodia (*arrows in C*). Small spots of stain can also be seen along the length of some filopodia (*arrowhead in C*). In growth cones with broad expanses of lamellipodia the staining was more intense in areas of the P domain that appeared to be ruffling at the time of freezing (*arrowheads in D*). The increased intensity of stain in the ruffles and the C domain may result from the increased fluorescence path length associated with these areas.

ferences may result from the fact that the antibody recognizes both G and F actin while rhodamine-phalloidin stains only F actin.

Immunofluorescence staining of growth cones with antibodies to myosin gave a unique pattern of staining. These observations are based upon 163 images of growth cones from seven different preparations. The staining was typically most intense in the C domain (in 82% of the growth cones that were observed), although staining was also present in the P domain (Fig. 5, *C* and *D*). Often the staining had a punctate pattern. However, very bright staining of the C domain often obscured this pattern in the photographs, as did slight changes in the plane of focus. Sometimes the spots of stain seemed to line up, as if aligned along filament bundles. However, this pattern was very subtle and difficult to demonstrate in the photographs that were obtained. The base of filopodia was often associated with especially bright spots of stain. Some filopodia also contained distinct spots of stain periodically along their length (Fig. 5 *C*). Neurites stained brightly along their entire length. In some growth cones containing broad areas of lamellipodia discrete ruffles stained brightly compared to the surrounding lamellipodial area (Fig. 5 *D*). This was in sharp contrast to the staining pattern seen with the anti-actin antibodies in lamellipodial type growth cones

(Fig. 5 *B*). The actin staining was intense throughout the lamellipodia and characteristically much less bright within the C domain. Frequently growth cones stained with the anti-myosin antibodies contained bright fluorescent spots in a transition zone between the P and the C domains. We tried to determine whether these brightly staining areas corresponded to the bright areas seen with the anti-actin or rhodamine-phalloidin staining by double labeling the same growth cone. However, the results were inconclusive because we were unable to prevent cross-reaction of the fluorescent secondary antibodies and the phalloidin staining did not work on freeze substituted cells. We do not know why phalloidin staining did not work after freeze substitution since it presumably has less of an effect on cell structure than traditional fixation and dehydration processes. However, removal of the hydration shell surrounding proteins undoubtedly causes conformational changes. Small changes that affect positions in the range of only Angstrom units might be sufficient to inactivate the binding site for even tightly binding agents such as phalloidin, although it would not be possible to see these changes with the best electron microscope techniques.

Immunoelectron Microscopy

A variety of methods were tried to localize myosin at the ultrastructural level. All attempts to use preembedment labeling procedures such as described by Langanger et al. (22), were unsuccessful because even mild fixation destroyed the antigenicity of myosin while permeabilization procedures that avoided fixation before labeling disrupted the organization normally seen in freeze-substituted growth cones by im-

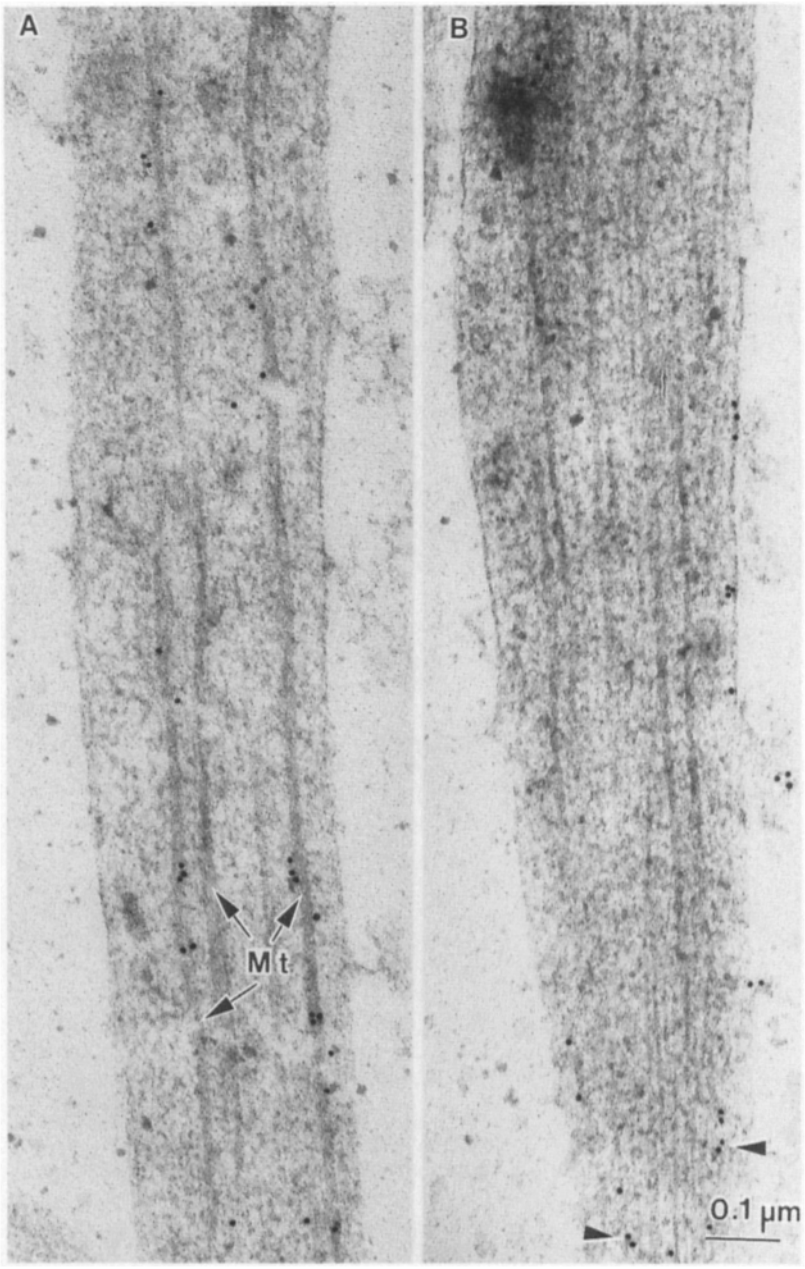

Figure 6. Immunogold labeling of microtubules (*A*) and myosin (*B*) on thin sections of rapid frozen, freeze-substituted neurites embedded in Lowicryl K11M. (*A*) A longitudinal section through a neurite incubated with an antiserum against tubulin followed by anti-rabbit IgG conjugated to 10-nm colloidal gold. Colloidal gold is closely associated with microtubules (*Mt*). (*B*) A slightly oblique longitudinal section through a neurite incubated with the antiserum against myosin followed by anti-rabbit IgG conjugated to 10-nm colloidal gold. Colloidal gold is not associated with microtubules but seems to be most prevalent just beneath the membrane surface, especially at the bottom of the picture (*arrowheads*) where the plane of section is about to leave the neurite. Both *A* and *B* were grid stained with uranyl acetate followed by potassium permanganate.

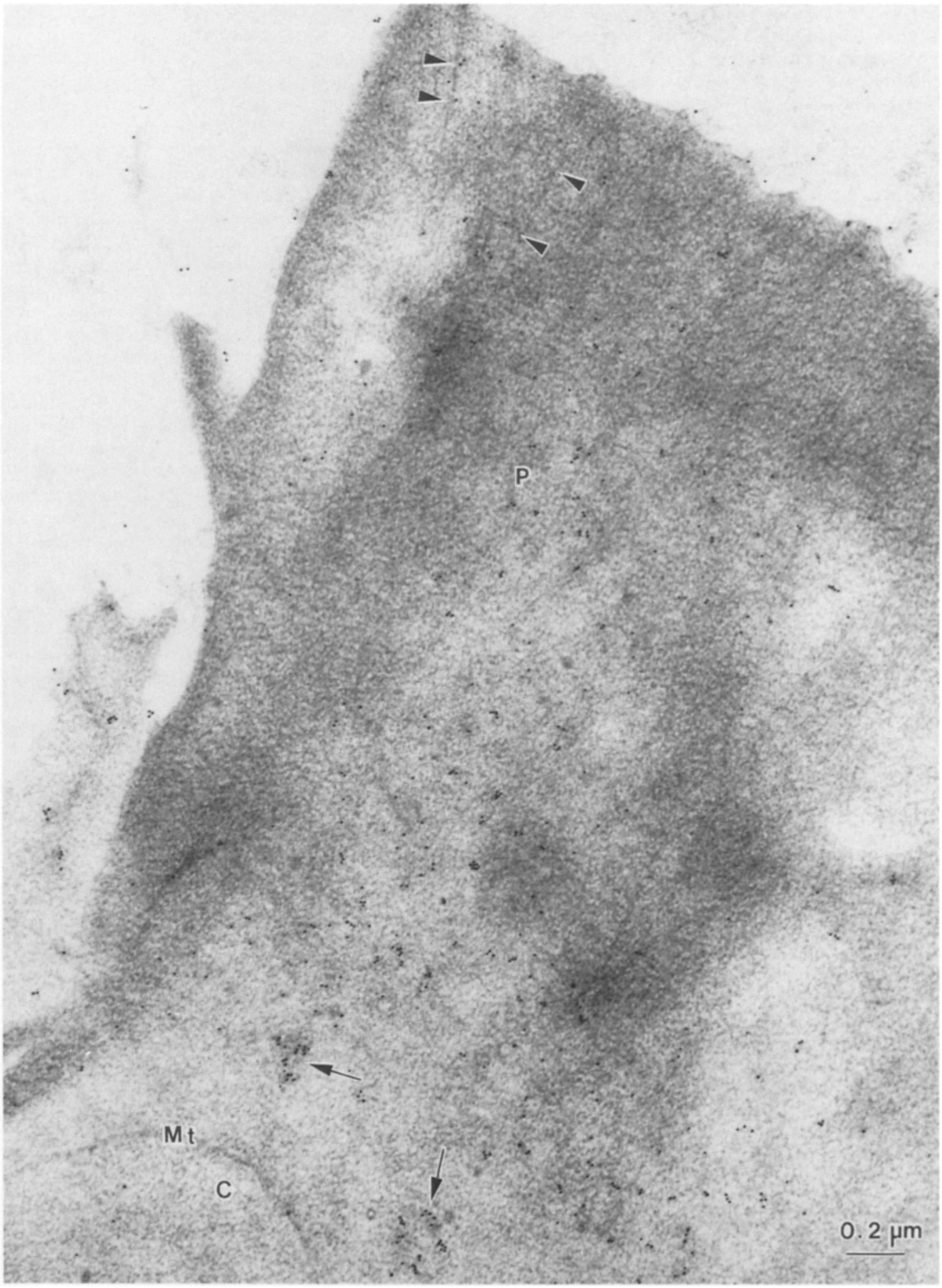

Figure 7. An en face section cut through a broadly spread lamellipodium that has been incubated with the antiserum against myosin followed by anti-rabbit IgG conjugated to 10-nm colloidal gold. Faintly stained filaments (*arrowheads*) radiate from the leading edge towards the C domain. The colloidal gold seems randomly distributed throughout the lamellipodium except at the transition region between the P and C domains. In this region aggregates of 15–20 gold particles (*arrows*) can be seen that are often associated with areas of increased staining or electron density. However, not all areas of increased electron density are associated with colloidal gold label. *Mt*, microtubule; *P*, peripheral domain; *C*, central domain. Grid stained with uranyl acetate.

munofluorescence. Attempts to label intact cells after freezing and freeze substitution were unsuccessful because even 5-nm gold particles were unable to penetrate into the cytoplasm. For this reason thin section postembedment labeling procedures on rapid frozen, freeze substituted cells were used.

The postembedment labeling method that was used has proven to be successful in other studies carried out by this laboratory to detect the distribution of acetylcholine receptors and associated proteins in Torpedo electroplaque cells and membrane fractions (Bridgman, P. C., unpublished results). To test the specificity of the labeling procedure for SCG neurons, a positive control was done. Microtubules are readily recognizable in the thin sections of Lowicryl K11M embedded neurites and growth cones. We therefore first used the antiserum against tubulin followed by a 10-nm colloidal gold-tagged second antibody to see if microtubules could be labeled. Gold particles were seen along neurites and at the base of growth cones. Often the gold particles were aligned on or in close proximity to microtubules suggesting that the labeling procedure was highly specific (Fig. 6 *A*). The resolution of postembedment labeling procedures employing the double antibody, colloidal gold technique is generally considered to be ~25 nm when using 10-nm gold particles. This is consistent with results we have obtained in other studies (Bridgman, P. C., unpublished results). To quantitate the percentage of microtubules that were labeled we counted the number of microtubules that were associated with at least one gold particle closer than 25 nm. 76% of microtubules were labeled according to this criterion (n = 228). In addition, gold particles were in low density in areas of neurites or growth cones without recognizable microtubules.

In comparison to the distribution of label seen using the anti-tubulin antiserum, the anti-myosin antiserum gave a completely different pattern of label. In neurites the label was confined almost exclusively to the area just beneath the plasma membrane (Fig. 6 *B*). In en face sections of growth cones the pattern of labeling was much more complex. The following observations are based upon 152 images of ~20 different growth cones from three separate preparations. In the P domain, especially within broadly spread lamellipodia, label was scattered throughout in a seemingly random manner (Fig. 7). The label did not seem to associate preferentially with filaments which presumably represent bundled actin filaments. In the transition zone between the P and C domains the label tended to be less uniformly scattered. Aggregations of 10–20 gold particles were common and were often associated with irregularly shaped darkly stained areas (Fig. 7). Some of the first sections which were cut so that they barely grazed beneath the bottom membrane surface of the P domain sometimes gave a higher density of labeling and larger numbers of aggregates than sections that were cut deeper into the cell cytoplasm (Fig. 8). Aggregations of label were commonly found immediately adjacent to the base of filopodia (Fig. 9 *A*). Label was also sometimes seen in small aggregates of several gold particles along the length of filopodia (not shown).

Within the C domain, label was present as scattered single gold particles, although aggregates of gold particles were also present (Fig. 9). These aggregates were often, though not always, associated with irregularly shaped darkly stained areas. Sometimes the aggregates of label were in close proximity to distinct filaments that may represent bundles of actin filaments. Occasionally label was seen adjacent to microtubules although this was not a consistent finding.

To determine if the concentration of label was different in the two domains we obtained quantitative values for the gold particle density from four growth cones (Table I). For the quantitation we selected only growth cones that were sectioned so that large portions of both the C and P domains could be seen on the same section. Only rarely was the plane of section oriented so that this was achieved. Although this limited the number of growth cones that could be used for quantitation, it was necessary because of the variation in absolute level of labeling and background from grid to grid which probably results from the plane of section and some variation in the efficiency of the blocking and washing procedures. As indicated in Table I, the average density of label was the same for both domains. On the same growth cones we compared the average density of aggregates per section for the two domains. An aggregate was arbitrarily defined as a minimum of 10 gold particles within a circle with a diameter of 0.25 μm. The peripheral region had an average of 0.12/μm^2 and the central region an average of 0.08/μm^2. This indicates that the concentration of aggregates is only slightly greater in the P domain. However, many of these aggregates (57%) were located in a zone adjacent (within 1.5 μm) to the C domain. Moreover, the volume of the C domain is greater because of its greater thickness, which is undoubtedly why the C domain stains brighter than the P domain with immunofluorescence.

Controls in which nonimmune serum were used or the primary antiserum was left out, showed a variable but relatively low background of colloidal gold label over growth cones (0.6–1.8 particles/μm^2). This background label was always distributed as scattered single (occasionally double) particles, never as aggregates.

Discussion

The organization of actin filaments in rapid frozen growth cones was roughly consistent with that which has been described by previous workers (24, 25). Actin filaments were highly concentrated in the P domain; they formed the core of filopodia and made up the supporting structure of lamellipodia. In lamellipodia they were occasionally tightly bundled but were more likely to be present as an overlapping meshwork. The individual filaments of both bundles and the meshwork were oriented so that they extended from the leading edge to the boundary with the C domain. The C domain also had actin filaments but in lower concentrations and usually the filaments were organized into bundles. The orientation of the actin filament bundles in the C domain was complex; sometimes they were oriented parallel with actin filaments in the P domain while in other cases they were perpendicular or at oblique angles. In addition to these features, there are two aspects of actin organization that have not been previously described or carefully considered.

First, actin filaments in the P domain sometimes terminate in distinct foci that are usually located about one third the distance back from the leading edge, in the transition region between the P and C domains. This may be important for the following reason. There is some evidence that actin filaments polymerize in a consistent orientation from the plasma membrane (37, 39). The barbed or fast growing end of the actin

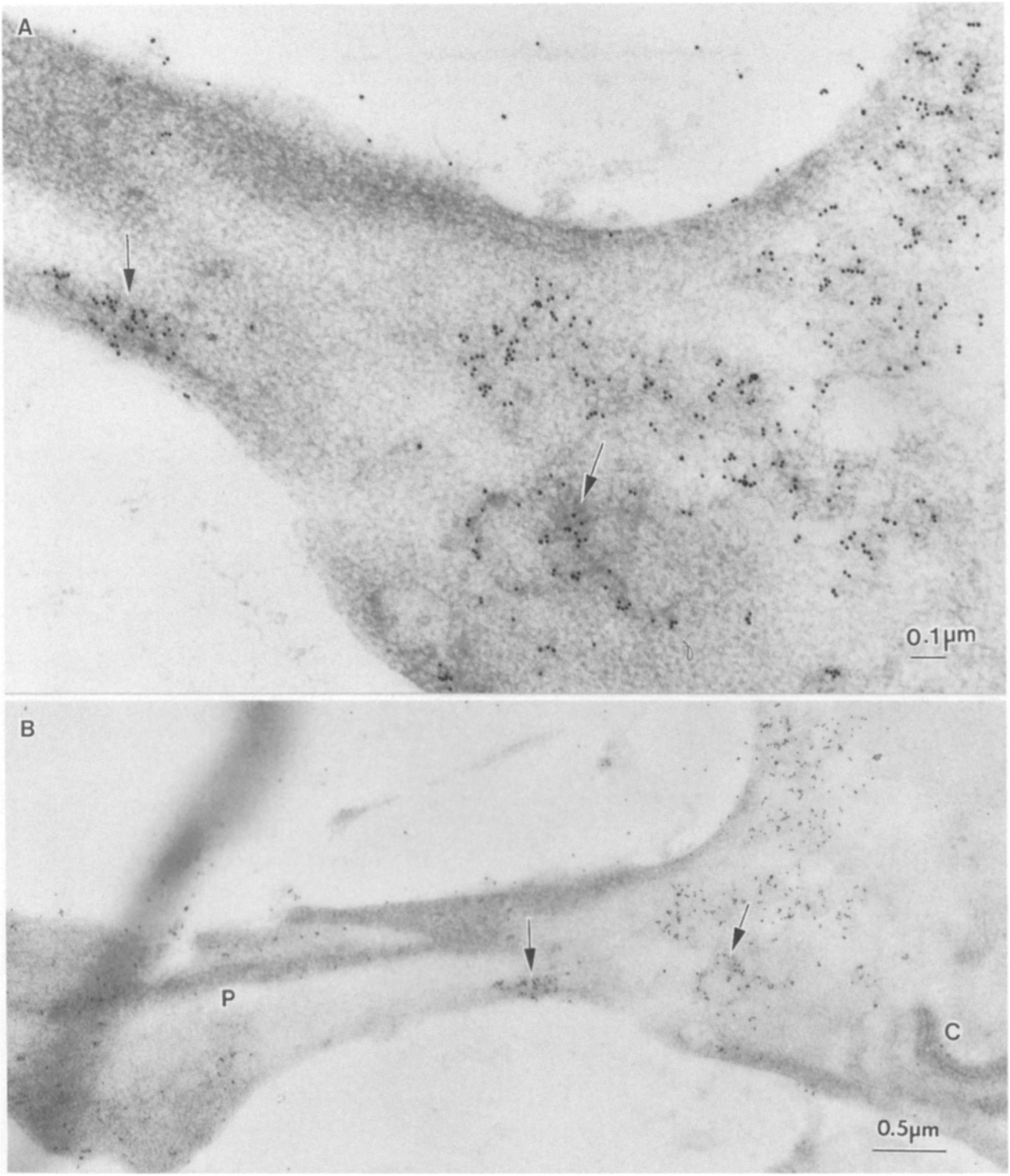

Figure 8. En face section through a different growth cone labeled as in Fig. 7 shown at high magnification (*A*) and a lower magnification (*B*) for orientation. (*A*) Discrete fairly large aggregates of anti-myosin colloidal gold label seem to be associated with dark staining areas of cytoplasm (*arrows*). A relatively high density of dispersed label is seen on the right hand side of the micrograph where the plane of section barely grazes beneath the membrane. An irregular meshwork of filamentous-like material is seen in these areas. (*B*) A lower magnification view of the same section shown in *A*. The peripheral extension on the left appears to expand to a lamellipodial-type projection. The aggregates (*arrows*) are at the base of the projection. The central portion of the growth cone can be seen on the right. Grid stained with uranyl acetate. *P*, peripheral domain; *C*, central domain.

filament is associated with the plasma membrane of the leading edge. We observed filaments extending from the leading edge to foci. This indicates that the foci may be consistently associated with the pointed end of actin filaments. Immunofluorescence of growth cones with antibodies to α actinin which is normally present in muscle cell Z lines has been

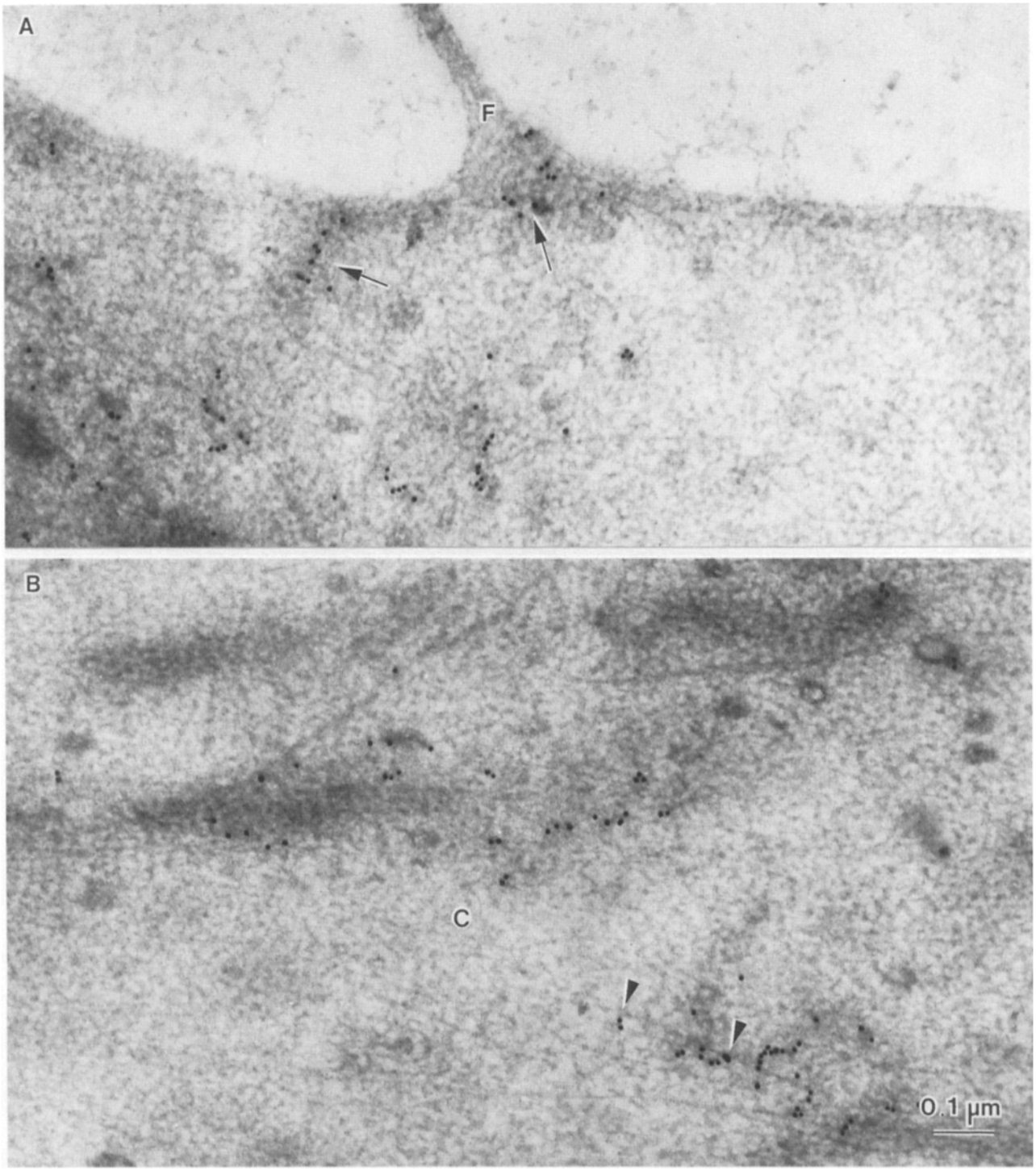

Figure 9. (*A* and *B*) En face sections, labeled as in Fig. 7, through two growth cones near their bases showing the C domain and in *A* an extension of a filopodium from the edge of the growth cone in this region. (*A*) Anti-myosin colloidal gold label is aggregated near the base of the filopodium (*arrows*) and in discrete dark areas within the C domain. (*B*) Deeper in the central domain, aggregates of the anti-myosin colloidal gold particles associate with dark staining regions and sometimes can be seen in close proximity to filaments (*arrowheads*). *C*, central domain. Grid stained with uranyl acetate.

reported to produce a staining pattern that is similar to the distribution of foci that we observe (36). These foci may therefore be analogous to the Z lines seen in muscle cells, although to confirm this double labeling experiments need to be done. There is, however, a discrepancy between the orientation of actin that we have inferred from our observations and the organization known to exist in muscle cells. Muscle cell Z lines are associated with the barbed end of actin filaments, not the pointed end. Direct determination of the orientation of growth cone actin filaments by HMM or SI

Table I. Density of Antimyosin Gold Particle Label in the P and C Domains on Thin Sections

	Particles/μm^2		
Growth cone No.	C Domain	P Domain	Background
1	12	11	0.8
2	9	8	0.5
3	24	33	7.0
4	18	15	4.0
Average	16	17	3.0

Thin sections cut so that the plane of section revealed large areas (>18 μm^2) of both P and C domains in a single growth cone were selected for quantitation. All sections were labeled with the rabbit anti-myosin antiserum at a 1:10 dilution followed by anti-rabbit IgG conjugated to 10-nm colloidal gold. Background counts were from cell-free regions immediately adjacent to the growth cones used for quantitation.

decoration needs to be done to solve this apparent contradiction. Although the polarity of the actin filaments that radiate from the foci still needs to be determined, the presence of the foci is intriguing for the following reason. Presumably, the actin filaments that extend from the leading edge to the foci are oriented with the opposite polarity relative to the orientation of the growth cone compared to those that extend from the base of the growth cone in the C domain and terminate at the foci. Consideration of actin filament polarity will be important for determining how the sliding of actin filaments or the production of tension is generated when actin undergoes interactions with myosin.

Second, it is apparent that growth cones that lack filopodia in our cultures also usually lack distinct actin bundles in the P domain. This indicates that advance of growth cones is not dependent upon filopodia formation or their underlying actin bundles, since the growth cones with broad lamellipodia, lacking filopodia, are among those that advance most rapidly in our culture system (3). This observation is important for at least two reasons. Filopodia have been implicated in the production of tension which has been thought to provide the traction necessary for the forward advance and guidance of the growth cone (5). In addition, it has been recently suggested that the growth of an axon occurs through a typical sequence of events that involves (*a*) extension of filopodia, (*b*) growth of veils between adjacent filopodia, (*c*) followed by advance of organelles (i.e., components of the C domain) into the veils (15). When filopodia are not readily evident, it was suggested that this was because they were being masked by the lamellipodia and would become apparent if the lamellipodia retracted. Although the role that filopodia are assumed to play in neurite elongation is vastly different in the two studies mentioned above, they both assume that filopodia are important for neurite elongation, contain core bundles of actin filaments, and that these bundles of filaments can be obscured by an advancing veil but nevertheless remain as distinct bundles. Our results suggest that this is not necessarily true because lamellipodia can exist without distinct filament bundles and are seen in growth cones associated with rapidly elongating neurites. This brings into question whether filopodia and the associated actin filament bundles play an important role in the growth process. Note, however, that the actin filaments in lamellipodia, whether organized in a meshwork or as loose bundles, are roughly parallel to the distinct actin bundles seen in growth cones with filopodia. This may indicate that the orientation of actin filaments in the leading edge is more important for growth cone advance than whether or not the filaments are bundled.

Details of myosin organization in growth cones of primary neurons have been sketchy and variable. Using immunofluorescence, Roisen et al. (34) and Kuczmarski and Rosenbaum (21) both reported diffuse staining while Shaw et al. (36) showed one picture of a punctate pattern of staining. One study has also described the immunofluorescence staining pattern seen in growth cones of PC12 cells (24). In this latter study, myosin staining was localized and appeared to overlap in position with the distribution of strong actin staining. Our results suggest that the pattern of myosin localization is complex. For instance, lamellipodia contained very high concentrations of actin filaments but the amount of myosin in lamellipodia was no different than that seen in the C domain and was apparently diffusely distributed, except perhaps at points where active ruffling was occurring. Myosin label was typically concentrated in distinct aggregates at the base of filopodia, in the P domain where it transitions into the C domain, and less frequently within the C domain itself. These aggregates of label may have functional importance if they represent associations of several molecules as bipolar filaments. The different number and exact locations of the aggregates seen in different growth cones indicates that myosin localization may change with the activity and shape of the growth cone. This is consistent with the activity of myosin in other nonmuscle cells; myosin filaments can form and then rapidly break down in response to the activity of the cell (40). It is apparent from the immunoelectron microscopy experiments that myosin may be more concentrated near the plasma membrane; cross sections showed more label just beneath the membrane and en face sections that just grazed beneath the membrane surface gave higher densities of label than those cut deeper into the cytoplasm.

The anti-myosin label which appeared as aggregates on thin sections were often associated with areas that stained dark compared to the surrounding area. The dark staining areas may be regions of substrate contact because contact regions often stain darker than adjacent regions (16). However, we have no direct evidence that this is indeed the case. We also considered whether these areas could be the same dark staining areas seen in whole mounts that represent foci of actin filaments. This seems unlikely because the actin filament foci were relatively small in number (3–10/growth cone) while the aggregates of myosin label were usually >10/growth cone. In any case, the presence of two different types of dark staining regions may explain why not all the dark staining regions are associated with aggregates of myosin label. As indicated above, the aggregates of myosin label could possibly represent bipolar filaments made up of a few myosin molecules. However, it is difficult to judge how many molecules could be represented by the amount of label that was observed. Although we know from rotary shadowing that the antiserum contains antibodies to several epitopes on the heavy chain (Bridgman, P. C., unpublished results), there are many unknowns associated with translating the labeling seen by rotary shadowing to that seen using postembedment labeling. For instance, it is likely that when the plane of section passes through a myosin molecule, only a small percentage of the epitopes per molecule are exposed on the surface of the section and available for reaction with antibodies.

The presence of myosin in growth cones raises the possibility that sliding of actin filaments and contractile activity contributes to the movements seen in locomoting growth cones. This needs to be discussed in the context of two recent findings.

First, growth cones can still elongate, although relatively slowly, under conditions in which most of the actin has been depolymerized (28). This elongation is characterized by disoriented growth. Evidence has accumulated that this actin-independent elongation may be microtubule based. This means that there is probably more than a single mechanism involved in neurite elongation and guidance (27). Thus actomyosin interaction may only be necessary for the higher rates of elongation seen under more physiological conditions and for determining the direction of growth.

Second, in several recent experiments the genetic expression of myosin has been suppressed in motile single cells by antisense RNA or gene conversion (13, 20). Surprisingly, in both studies, the cells remained viable under certain culture conditions and still showed movement. However, the movement was abnormal, it was greatly slowed and normal chemotaxis was disrupted, although locomotion could still occur to some extent. This indicates that conventional myosin is probably not necessary for protrusive movements and some of the forces that can lead to motility. On the other hand, since locomotion was greatly slowed and the ability to steer in the correct direction abnormal, it is possible that conventional myosin is necessary or involved in the processes essential for rapid movements in a coordinated manner.

These different factors may be integrated into a reasonable explanation of how neurite growth occurs in our system if one accepts that elongation may involve a number of mechanisms operating simultaneously. This implies that a high rate of directed growth occurs only when these mechanisms are all operating in concert. These mechanisms would possibly include: (*a*) assembly and/or sliding of microtubules; (*b*) fast transport of membraneous organelles into the growth cone; (*c*) membrane addition at the growth cone; (*d*) protrusion of lamellipodia and filopodia through assembly of the actin cytoskeleton; (*e*) substrate attachment; (*f*) sliding of actin filaments through interaction with myosin in the peripheral region resulting in traction; and (*g*) contractile activity generated through the interaction of actin and myosin at the base of the growth cone resulting in consolidation into the neurite. In particular, these last three mechanisms may be necessary (but not sufficient) for the generation of rapid growth and steering of the neurite.

Although we feel that the interaction of actin and myosin may contribute to the rapid locomotion of growth cones in our system, it seems premature to construct a more detailed model of how this activity contributes to the motility. More information is needed on the structure and regulation of the growth cone actin-based cytoskeleton and how it interacts on a molecular level with myosin before this can be done satisfactorily. For example, a single headed globular form of myosin (myosin I) has been discovered in Acanthamoeba (29) and a similar form may also exist in vertebrate cells (12). This novel form of myosin has been shown to have shared epitopes with conventional myosin (myosin II) (19). Although our antiserum showed no detectable cross-reactivity with any rat nerve proteins other than a 205-kD protein that presumably represents the heavy chain of a traditional type of myosin (myosin II), the possibility still remains that a myosin I–like molecule could exist in nerve and be responsible for some aspects of the motility that is observed.

We wish to thank Grady Phillips and Mary Kordyban for expert technical help and Dr. Naomi Kleitman for comments on the manuscript. We also thank Dr. Peter Cook for help with the HVEM.

This research was supported by a program project grant, NS15070, and we also acknowledge the support of the Integrated Microscopy Resource for Biomedical Research at the University of Wisconsin, Madison.

Received for publication 16 May 1988, and in revised form 6 September 1988.

References

1. Aletta, J. M., and L. A. Greene. 1988. Growth cone configuration and advance: a time-lapse study using video-enhanced differential contrast microscopy. *J. Neurosci.* 8:1425–1435.
2. Ashford, A. E., W. G. Allaway, F. Gubles, A. Lennon, and J. Sleegers. 1986. Temperature control in Lowicryl K4M and glycol methacrylate during polymerization: is there a low-temperature embedding method? *J. Microsc. (Oxf.).* 144:107–126.
3. Argiro, V., M. B. Bunge, and M. I. Johnson. 1984. Correlation between growth form and movement and their dependence on neuronal age. *J. Neurosci.* 4:3051–3062.
4. Bray, D. 1979. Mechanical tension produced by nerve cells in tissue culture. *J. Cell Sci.* 37:391–410.
5. Bray, D. 1982. Filopodial contraction and growth cone guidance. *In* Cell Behavior. R. Bellairs, A. Curtis, and G. Dunn, editors. Cambridge University Press, Cambridge, England. 299–317.
6. Bray, D. 1984. Axonal growth in response to experimentally applied mechanical tension. *Dev. Biol.* 102:379–389.
7. Deleted in proof.
8. Bridgman, P. C., and T. S. Reese. 1984. The structure of cytoplasm in directly frozen cultured cells. I. Filamentous meshworks and the cytoplasmic ground substance. *J. Cell Biol.* 99:1655–1668.
9. Deleted in proof.
10. Bridgman, P. C., B. Kachar, and T. S. Reese. 1986. The structure of cytoplasm in directly frozen cultured cells. II. Cytoplasmic domains associated with organelle movements. *J. Cell Biol.* 102:1510–1521.
11. Carlemalm, E., W. Villiger, J. A. Hobot, J.-D. Acetarin, and E. Kellenberger. 1985. Low temperature embedding with Lowicryl resins: two new formulations and some applications. *J. Microsc. (Oxf.).* 140:55–63.
12. Conzelman, K. A., and M. S. Mooseker. 1987. The 110-kD protein-calmodulin complex of the intestinal microvillus is an actin-activated MgATPase. *J. Cell Biol.* 105:313–324.
13. De Lozanne, A., and J. A. Spudich. 1987. Disruption of the Dictyostelium myosin heavy chain gene by homologous recombination. *Science (Wash. DC).* 236:1086–1091.
14. Forscher, P., L. K. Kaczmarek, J. Buchanan, and S. J. Smith. 1987. Cyclic AMP induces changes in distribution and transport of organelles within growth cones of Aplysia bag cell neurons. *J. Neurosci.* 7:3600–3611.
15. Goldberg, D. J., and D. W. Burmeister. 1987. Stages in axon formation: observations of growth of Aplysia axons in culture using video-enhanced contrast-differential interference contrast microscopy. *J. Cell Biol.* 103:1921–1932.
16. Heath, J. P., and G. A. Dunn. 1978. Cell to substratum contacts of chick fibroblasts and their relation to the microfilament system. A correlated interference-reflexion and high-voltage electron-microscope study. *J. Cell Sci.* 29:197–212.
17. Heuser, J. E., T. S. Reese, M. J. Dennis, Y. Jan, L. Jan, and L. Evans. 1979. Synaptic vesicle exocytosis captured by quick freezing and correlated with quantal transmitter release. *J. Cell Biol.* 81:275–300.
18. Johnson, M. I., and V. Argiro. 1983. Techniques in the tissue culture of rat sympathetic neurons. *Methods Enzymol.* 103:334–347.
19. Kiehart, D. P., D. A. Kaiser, and T. D. Pollard. 1984. Monoclonal antibodies demonstrate limited structural homology between myosin isozymes from acanthamoeba. *J. Cell Biol.* 99:1002–1014.
20. Knecht, D. A., and W. F. Loomis. 1987. Antisense RNA inactivation of myosin heavy chain gene expression in Dictyostelium discoideum. *Science (Wash. DC).* 236:1081–1086.
21. Kuczmarski, E. R., and J. L. Rosenbaum. 1979. Studies on the organization and localization of actin and myosin in neurons. *J. Cell Biol.* 80:356–371.
22. Langanger, G., M. Moeremans, G. Daneels, A. Sobieszek, M. DeBrabander, and J. DeMey. 1986. The molecular organization of myosin in stress fibers of cultured cells. *J. Cell Biol.* 102:200–209.
23. Letourneau, P. C. 1975. Possible roles for cell-to-substratum adhesion in neuronal morphogenesis. *Dev. Biol.* 44:77–91.
24. Letourneau, P. C. 1981. Immunocytochemical evidence for colocalization

in neurite growth cones of actin and myosin and their relationship to cell-substratum adhesions. *Dev. Biol.* 85:113–122.
25. Letourneau, P. C. 1983. Differences in the organization of actin in the growth cones compared with the neurites of cultured neurons from chick embryos. *J. Cell Biol.* 97:963–973.
26. Letourneau, P. C. 1985. Axonal growth and guidance. *In* Molecular Basis of Neural Development. G. M. Edelman, W. E. Gall, and W. M. Cowen, editors. Neuroscience Research Foundation, New York. 269–293.
27. Letourneau, P. C., T. A. Shattuck, and A. H. Ressler. 1987. "Pull" and "Push" in neurite elongation: observations on the effects of different concentrations of cytochalasin B and Taxol. *Cell Motil. Cytoskeleton.* 8:193–209.
28. Marsh, L., and P. C. Letourneau. 1984. Growth of neurites without filopodial or lamellipodial activity in the presence of cytochalasin B. *J. Cell Biol.* 99:2041–2047.
29. Maruta, H., H. Gadasi, J. C. Collins, and E. D. Korn. 1979. *J. Biol. Chem.* 254:3624–3630.
30. Peleg, I., Il. Kahane, A. Eldor, U. Groschel-Stewart, J. Mestan, and A. Muhlrad. 1983. Structural properties of myosin from the particulate fraction of human blood platelets. *J. Biol. Chem.* 258:9290–9295.
31. Deleted in proof.
32. Pollard, T. D., S. M. Thomas, and R. Niederman. 1974. Human platelet myosin. I. Purification by a rapid method applicable to other nonmuscle cells. *Anal. Biochem.* 60:258–266.
33. Rogers, S. L., P. C. Letourneau, S. L. Palm, J. McCarthy, and L. T. Furcht. 1983. Neurite extension by peripheral and central nervous system neurons in response to substratum-bound fibronectin and laminin. *Dev. Biol.* 98:212–220.
34. Roisen, F., M. Inczedy-Marcsek, L. Hsu, and W. Yorke. 1978. Myosin: immunofluorescent localization in neuronal and glial cultures. *Science (Wash. DC).* 31:1445–1448.
35. Deleted in proof.
36. Shaw, G., M. Osborn, and K. Weber. 1981. Arrangement of neurofilaments, microtubules and microfilament-associated proteins in cultured dorsal root ganglia cells. *Eur. J. Cell Biol.* 24:20–27.
37. Small, J. V., G. Isenber, and J. E. Celis. 1978. Polarity of actin at the leading edge of cultured cells. *Nature (Lond.).* 272:638–639.
38. Terasaki, M., L. B. Chen, and K. Fujiwara. 1986. Microtubules and the endoplasmic reticulum are highly interdependent structures. *J. Cell Biol.* 103:1557–1568.
39. Wang, Y.-L. 1985. Exchange of actin subunits at the leading edge of living fibroblasts: possible role of treadmilling. *J. Cell Biol.* 101:597–602.
40. Yumura, S., and Y. Fukui. 1985. Reversible cyclic AMP-dependent change in distribution of myosin thick filaments in Dictyostelium. *Nature (Lond.).* 314:194–196.